CHEMISTRY
A EUROPEAN JOURNAL

DOI: 10.1002/chem.200600124

NIR Lanthanide Luminescence by Energy Transfer from Appended Terpyridine–Boradiazaindacene Dyes

Raymond F. Ziessel,*[a] Gilles Ulrich,[a] Loïc Charbonnière,[a] Daniel Imbert,[b] Rosario Scopelliti,[b] and Jean-Claude G. Bünzli*[b]

Abstract: Mononuclear trivalent lanthanide complexes with formula $[Ln(L)(NO_3)_3]$ [in which L = 4,4-difluoro-8-(2′:2″;6″:2‴-terpyridin-4″-yl)-1,3,5,7-tetramethyl-2,6-diethyl-4-bora-3a,4a-diaza-s-indacene (Boditerpy)] are reported for Ln = Yb, Nd, Er, La and Gd. According to the crystal structure of the Yb complex, the lanthanide ion is bound to the terdentate terpyridine and the inner coordination sphere of the nine-coordinate lanthanide ion is completed by three bidentate nitrate anions. The coordination polyhedron can be described as a distorted tricapped antiprism. The terpyridine chelate is almost planar and tilted by nearly 60° from the indacene subunit. FT-IR spectra confirm the bidentate binding mode of the nitrate anions for the other complexes. NMR and ES-MS spectra (through characteristic isotopic patterns) confirm the chemical formulation. The complexes have high molar absorption coefficients in the visible spectral region ($65\,000\,M^{-1}cm^{-1}$ at 529 nm) and display sizeable NIR luminescence (900 to 1600 nm, for Ln = Yb, Nd and Er), upon irradiation through the electronic state of the indacene moiety at 514 nm. Crystal-field splitting was analysed at low temperature. The quantum yield of the Yb solution (10^{-4} M) in dichloromethane amounts to 0.31 %, corresponding to a sensitisation efficacy of the ligand of ca. 63 %.

Keywords: dyes/pigments · energy transfer · IR spectroscopy · lanthanides · luminescence

Introduction

The remarkable transparency of biological tissues to electromagnetic radiation in the range 0.8–1.3 μm allows the development of smaller, more penetrable probes for imaging by using near-infrared (NIR) light.[1,2] Additionally, the need for luminescent polymers for optical amplifiers[3] and light-emitting diodes working in the telecommunication window (1–1.6 μm)[4] has inspired extensive efforts for the development of such luminescent materials. In this context, NIR lanthanide-based emitters are of substantial interest in view of their specific spectroscopic properties, namely narrow and easily recognisable emission lines and relatively long lifetimes of their excited states, relative to those of organic chromophores. The last feature allows the use of time-resolved spectroscopy in analytical procedures, thus enhancing considerably the signal-to-noise ratio and consequently the sensitivity of luminescent analyses and imaging. The lanthanide ions of interest for the aforementioned applications are: Pr^{III}, emitting mainly at 1.03 and 1.33 μm ($^1G_4 \rightarrow {}^3H_{4,5}$ transitions), Nd^{III} with fluorescence lines at 0.88, 1.06 and 1.33 μm ($^4F_{3/2} \rightarrow {}^4I_{9/2}$, $^4I_{11/2}$, $^4I_{13/2}$ transitions), Er^{III} with an emission at 1.53 μm ($^4I_{13/2} \rightarrow {}^4I_{15/2}$ transition) and Yb^{III} which gives off light at 0.98 μm ($^2F_{5/2} \rightarrow {}^2F_{7/2}$ transition), see Figure 1. Since Pr^{III} luminescence in the NIR range is usually faint for molecular compounds, owing to its simultaneous visible-range emission from the $^1D_2$ and $^3P_0$ levels, we concentrate here on the three other NIR-emitting lanthanide ions.

Intraconfigurational f–f transitions have faint oscillator strengths and therefore a sensitisation process is needed to pump energy into the Ln^{III} ions, that is, the immediate environment of the Ln^{III} ions harvests light and transfers its energy onto the metal ion itself. For molecular coordination

[a] Dr. R. F. Ziessel, Dr. G. Ulrich, Dr. L. Charbonnière
Laboratoire de Chimie Moléculaire, École de Chimie Polymères, Matériaux (ECPM)
Université Louis Pasteur-CNRS (UMR 7509)
25 rue Becquerel, 67008 Strasbourg Cedex (France)
Fax: (+33) 390-242-635
E-mail: ziessel@chimie.u-strasbg.fr

[b] Dr. D. Imbert, Dr. R. Scopelliti, Prof. J.-C. G. Bünzli
École Polytechnique Fédérale de Lausanne (EPFL),
Laboratory of Lanthanide Supramolecular Chemistry
1015 Lausanne (Switzerland)
Fax: (+41) 21-693-9825
E-mail: jean-claude.bunzli@epfl.ch

Supporting information for this article is available on the WWW under http://www.chemeurj.org/ or from the author.

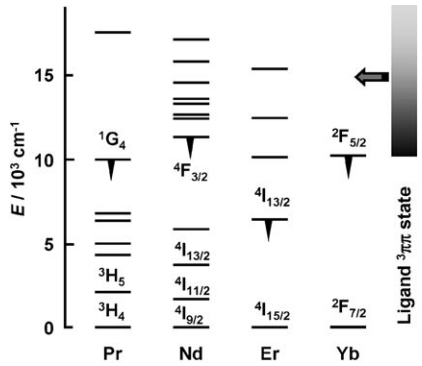

Figure 1. Partial energy diagram of some NIR-emitting lanthanide ions;[5] the luminescent state is indicated by an arrow and the end state is labelled.

compounds, this process usually involves the triplet state of the ligand,[6] but singlet-state sensitisation has been invoked in few cases.[7] Alternatively the excited states of the Ln^{III} ions can also be populated through directional energy transfer from d transition metal ions in heteropolymetallic edifices.[2,5,8–10] In this work, we resort to the first strategy and from the energy diagram shown in Figure 1, one sees that a ligand with a triplet-state energy in the range 10–18000 cm^{-1} would be an adequate sensitiser for the chosen Ln^{III} ions, as has been demonstrated with a podand fitted with 8-hydroxiquinolinates, for which the triplet state emission extends from 450 to 650 nm (22200–15400 cm^{-1}).[11] Tetraphenylporphyrin,[12] terphenyl,[13] pyrene[14] and triazolophthalazine[15] derivatives, as well as various dyes such as fluorescein derivatives,[16] have also been proposed to sensitise the NIR-emitting lanthanide ions. Despite this diversity, the quantum yields obtained remain modest, typically on the order of 10^{-3} to 10^{-2} for Yb^{III} and of 10^{-3} to 10^{-4} for Nd^{III} (except in coordination polymers for which a few percents can be obtained), while corresponding data for Er^{III} are even much smaller.[2,5] Therefore, there is a need for exploring the efficiency of new chromophores. We have consequently prepared a terpyridine-based difluoroborondipyrromethene dye (Boditerpy) that combines a high molar absorption coefficient, high fluorescence quantum yields, chemical and photochemical stability in solution and in the solid state under various stresses, and redox activity.[17] The uncomplexed ligand (L) is a singlet emitter at 540 nm (18500 cm^{-1}) and displays triplet state emission in the spectral range 750–800 nm (12500–13300 cm^{-1}) when complexed with transition metal ions.[18] We report here on the complexes formed by this ligand with NIR-emitting lanthanide ions, as well as on their solution and photophysical properties.

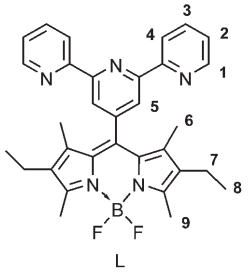

L

Abstract in French: *Des complexes mononucléaires d'ions lanthanides trivalents de formule générique [Ln(L)(NO$_3$)$_3$], ou L = 4,4-difluoro-8-(2′:2″;6″:2‴-terpyridine-4″-yl)-1,3,5,7-tétraméthyl-2,6-diéthyl-4-bora-3a,4a-diaza-s-indacène (Boditerpy) avec Ln = Yb, Nd, Er, La, et Gd ont été préparés et étudiés. La structure cristalline du complexe d'ytterbium confirme la coordination de l'ion lanthanide sur le fragment terpyridine et la première sphère de coordination du lanthanide est complétée par trois anions nitrates bidentés. Le polyèdre de coordination est un antiprisme tricappé distordu. Le chélate terpyridine est quasiment plan et incliné de 60° par rapport à l'indacène. La résonance magnétique nucléaire et la spectrométrie de masse par électro-spray confirment la formulation chimique des complexes obtenus en solution. Les complexes isolés absorbent fortement dans le visible (65000 $M^{-1}cm^{-1}$ à 529 nm) et émettent de la lumière dans le proche infra-rouge (900–1600 nm, Ln = Yb, Er et Nd) par irradiation dans la sous-unité indacene à 514 nm. A basse température l'influence du champ cristallin sur la dégénérescence des niveaux électroniques a également été mise en évidence. Le rendement quantique d'une solution de complexe d'ytterbium à 10^{-4} M dans le dichlorométhane est de 0,31 % et correspond à une efficacité calculée de transfert d'énergie de l'indacène vers l'état émissif de l'Yb de 63 %. Les perspectives de ce travail sont discutées à la lumière des résultats obtenus.*

Experimental Section

General methods: The 200 MHz (^{1}H) NMR spectra were recorded at room temperature by using perdeuterated solvents as internal standards: δ(H) are given in ppm relative to residual protiated solvent. An electrospray MS Agilent MSD-analytical apparatus in positive mode with an automatic calibration was used with dichloromethane as solvent. Simulations were performed with a Bruker Daltonics Data Analysis under the simulate isotopic patterns routine. FT-IR spectra were recorded on thin films, prepared with a drop of dichloromethane, and evaporated to dryness on KBr pellets.

Materials and reagents: The lanthanide salts were purchased from Aldrich, and the purity of all reagents grade materials were adequate as received. Analytical grade solvents sufficed in all cases. Ligand L was prepared as previously described.[17] IR (KBr, Figure S1, in the Supporting Information); $\tilde{\nu}$ = 2925 (m), 1539 (ν_{CN}, s), 1465 (m), 1392 (m), 1319 (m), 1261 (w), 1189 (s), 1058 (m), 976 cm^{-1} (m).

General procedure: The preparation of the complexes began with the dissolution of L (0.050 g, 0.0935 mmol) in anhydrous THF (10 mL) followed by the dropwise addition of a solution of $Ln(NO_3)_3{\cdot}6H_2O$ (1.2 equiv, 0.112 mmol) in THF (2 mL). Immediately after mixing the colour of the solution turned deep red; most of the ligand fluorescence was quenched when the solution is irradiated with a bench UV lamp at 365 nm. After a couple hours of stirring at RT, anhydrous diethyl ether (5 mL) and large excess of pentane (50 mL) were successively added. The resulting deep red solid was recovered by centrifugation and washed with a diethyl ether and pentane 1:1 v/v solvent mixture. The crude material was dissolved in dichloromethane and the resulting solution was filtered over celite and hexane was carefully added in order to avoid precipitation. Slow evaporation of the solvent resulted in the precipitation of deep-red crystals. Ultimate re-crystallisation by slow evaporation of dichloromethane from a dichloromethane/cyclohexane/ether solution afforded the pure complexes.

Data for $[La(L)(NO_3)_3]\cdot 3H_2O$: 0.068 g, 80% yield; ^{1}H NMR (200 MHz, $CDCl_3$): $\delta = 0.98$ (t, $^3J = 7.5$ Hz, 6H), 1.43 (s, 6H), 2.31 (br q, $J = 7.4$ Hz, 4H), 2.57 (s, 6H), 7.62 (br t, $^3J = 5.5$ Hz, 2H), 7.97–8.09 (m, 4H), 8.18 (s, 2H), 9.03 ppm (br d, $^3J = 4.5$ Hz, 2H); ESI-MS (CH_2Cl_2/THF positive mode): m/z: 798.2 $[M-NO_3]^+$, 536.2 $[L+H]^+$, 368.1 $[M-2NO_3]^{2+}$; IR (KBr): $\tilde{\nu} = 2914$ (m), 1539 (m), 1479 (br, s, ν_{NO}), 1312 (s), 1293 (s, ν_{NO}), 1186 (s), 1028 (w), 974 cm^{-1} (w); elemental analysis calcd (%) for $C_{32}H_{32}N_8O_9BF_2La\cdot 3H_2O$ (914.42): C 42.03, H 4.19, N, 12.25; found: C 41.76, H 3.96, N 11.67.

Data for $[Nd(L)(NO_3)_3]\cdot H_2O$: 0.080 g, 94% yield; ^{1}H NMR (200 MHz, CD_2Cl_2, all peaks are broad): $\delta = 0.88$ (6H), 1.26 (6H), 2.69–2.92 (m, 10H), 3.14 (2H), 5.64 (2H), 7.35 (2H), 9.27 (2H), 10.27 ppm (2H); ESI-MS (CH_2Cl_2/THF positive mode): m/z: 803.2 $[M-NO_3]^+$, 369.5 $[M-2NO_3]^{2+}$; IR (KBr): $\tilde{\nu} = 2925$ (m), 1733 (w), 1601 (w), 1538 (m), 1514 (m), 1472 (s, ν_{NO}), 1410 (m), 1307 (s), 1292 (s, ν_{NO}), 1193 (s), 1077 (w), 1035 (w), 977 cm^{-1} (w); elemental analysis calcd (%) for $C_{32}H_{32}N_8O_9BF_2Nd\cdot H_2O$ (883.71): C 43.49, H 3.88, N 12.68; found: C 43.21, H 3.56, N 12.43.

Data for $[Gd(L)(NO_3)_3]\cdot 2H_2O$: 0.066 g, 77% isolated yield; ESI-MS (CH_2Cl_2/THF positive mode): m/z: 817.2 $[M-NO_3]^+$, 377.5 $[M-2NO_3]^{2+}$; IR (KBr): $\tilde{\nu} = 2923$ (m), 1599 (w), 1540 (m), 1471 (s, ν_{NO}), 1411 (w), 1295 (s, ν_{NO}), 1189 (s), 1030 (w), 976 cm^{-1} (w); elemental analysis calcd (%) for $C_{32}H_{32}N_8O_9BF_2Gd\cdot 2H_2O$ (914.74): C 42.02, H 3.97, N 12.25; found: C 41.66, H 3.44, N 11.97.

Data for $[Er(L)(NO_3)_3]\cdot 2H_2O$: 0.071 g, 82% isolated yield; ESI-MS in CH_2Cl_2/THF positive mode: m/z: 825.2 $[M-NO_3]^+$, 381.5 $[M-2NO_3]^{2+}$; IR (KBr): $\tilde{\nu} = 2928$ (m), 1738 (w), 1615 (w), 1601 (w), 1545 (m), 1479 (s, ν_{NO}), 1416 (w), 1372 (w), 1321 (s), 1289 (s, ν_{NO}), 1194 (s), 1061 (w), 1033 (w), 979 cm^{-1} (w); elemental analysis calcd (%) for $C_{32}H_{32}N_8O_9BF_2Er\cdot 2H_2O$ (924.75): C 41.56, H 3.92, N 12.12; found: C 41.29, H 3.64, N 11.90.

Data for $[Yb(L)(NO_3)_3]\cdot H_2O$: 0.079 g, 93% isolated yield; ^{1}H NMR (200 MHz, CD_2Cl_2): $\delta = -4.78$ (s, 6H), −0.23 (t, $^3J = 7.5$ Hz, 6H), 0.81 (q, $^3J = 7.5$ Hz, 4H), 1.48 (br s, 6H + 2H), 9.30 (d, $^3J = 7.5$ Hz, 2H), 15.26 (br t, $J = 7.3$ Hz, 2H), 22.79 (br s, 2H), 70.13 (br s, 2H); ESI-MS (CH_2Cl_2/THF positive mode): m/z: 833.1 $[M-NO_3]^+$, 385.0 $[M-2NO_3]^{2+}$; IR (KBr, Figure S1, in the Supporting Information): $\tilde{\nu} = 2923$ (m), 1615 (w), 1600 (w), 1539 (m), 1519 (m) 1478 (s, ν_{NO}), 1416 (m), 1294 (s, ν_{NO}), 1277 (s), 1190 (s), 1015 (m), 976 cm^{-1} (m); elemental analysis calcd (%) for $C_{32}H_{32}N_8O_9BF_2Yb\cdot H_2O$ (912.51): C 42.12, H 3.76, N 12.28; found: C 41.87, H 3.45, N 11.81.

X-ray crystal structure determination of $[Yb(L)(NO_3)_3]\cdot H_2O$: Data collection was performed at 140(2) K with $Mo_{K\alpha}$ radiation on an Oxford Diffraction diffractometer with kappa geometry and equipped with a Sapphire CCD detector. Data reduction and cell refinement was performed by CrysAlis RED.[19] Data were corrected for absorption by using an empirical method (DELABS[20]). The structure was solved with ab initio direct methods and refined by full-matrix least-squares on F^2 with all non-hydrogen atoms anisotropically defined. No particular problem was encountered during the stages of refinement. Space group determination, structure refinement and graphical representation were carried out with the SHELXTL software package[21] (Table 1).

Physicochemical measurements: UV/Vis absorption spectra were measured on a Perkin–Elmer Lambda 900 spectrometer by using quartz Suprasil® cells of 0.2 and 1 cm path length. The equipment and experimental procedures for luminescence measurements in the visible range have been published previously.[22] Excitation of the finely powdered samples was achieved by a 450 W xenon high-pressure lamp coupled with a monochromator or a Coherent Innova argon laser. For the emission in the NIR, the emitted light was analysed at 90° with a Spex 1870 single monochromator with 950 g mm^{-1} holographic gratings blazed at 900 nm. Light intensity was measured with a Jobin Yvon DSS-IGA020 L solid-state InGaAs detector cooled to 77 K, in a LN2 housing including an elliptical mirror (90° beam path, range 800–1600 nm) and coupled to a Jobin Yvon SpectrAcq2 data acquisition system. The emission spectra were corrected for the instrumental function. Luminescent lifetimes were measured by using excitation provided by a Quantum Brillant Nd:YAG laser equipped with frequency doubler, tripler and quadrupler as well as with an OPOTEK MagicPrism™ OPO crystal. The output signal of the photomultiplier was fed into a Stanford Research SR-430 multichannel scaler and transferred to a PC. Lifetimes are averages of three independent determinations. Quantum yields were determined using a Spex Fluorolog FL-3-22 fluorimeter; for the ions emitting in the NIR region, the spectrometer was fitted with an additional single-grating monochromator FL-1004 equipped with an InGaAs detector cooled at 77 K. The quantum yields were calculated by using Equation (1), in which x refers to the sample and r to the reference; A is the absorbance, n the refractive index and D the integrated emitted intensity.

$$\frac{Q_x}{Q_r} = \frac{A_r n_x^2 D_x}{A_x n_r^2 D_r} \quad (1)$$

Rhodamine 6G in water (absolute quantum yield = 0.76)[23] was used as reference for the ligand-centred fluorescence (estimated error ±10%). The emission spectra were recorded at the same excitation wavelength, 488 nm with absorbance between 0.035 and 0.04. Quartz Suprasil® cells with 1 cm path length were used for these measurements. $[Yb(tta)_3(H_2O)_2]$ in toluene ($Q = 0.35\%$; tta = thenoyltrifluoroacetylacetonate)[24] was used as reference for the NIR-emitting ions (estimated error ±10%). Three independent measurements were performed, first at the same wavelength (341 nm) with $A = 0.18$–0.20 and then at different wavelengths (341 nm for the reference, 405 and 499 nm for the complexes) with $A = 0.03$ and 0.07, respectively. Quartz Suprasil® cells with 0.2 cm path length were used for these measurements.

Table 1. Summary of crystal data, intensity measurements, and structure refinement details for $[Yb(L)(NO_3)_3]$.

formula	$C_{32}H_{32}BF_2N_8O_9Yb$	M_r	894.51
T [K]	140(2) K	λ [Å]	0.71073
crystal system	monoclinic	space group	$P2_1/n$
a [Å]	8.8313(7)	α [°]	90
b [Å]	28.1514(18)	β [°]	105.238(7)
c [Å]	13.7974(11)	γ [°]	90
V [Å^3]	3309.6(4)	Z	4
ρ [Mg m^{-3}]	1.795	μ [mm^{-1}]	2.906
$F(000)$	1780	crystal size [mm^3]	0.28 × 0.14 × 0.09
θ range [°]	3.14–25.03	index ranges	$-10 \le h \le 10$ $-33 \le k \le 33$ $-16 \le l \le 16$
reflns collected	18918	independent reflns	5549 [R(int) = 0.0468]
Completeness to $\theta = 25.03°$ [%]	95.0	absorption correction	empirical (DELABS)
max/min transmission	0.828/0.469	refinement method	full-matrix least-squares on F^2
data/restraints/parameters	5549/0/478	goodness-of-fit on F^2	1.076
final R indices [$I > 2\sigma(I)$]	$R1 = 0.0353$, $wR2 = 0.0808$	R indices (all data)	$R1 = 0.0477$, $wR2 = 0.0873$
largest diff. peak/hole [e Å^{-3}]	1.843/−1.468		

Results and Discussion

The lanthanide complexes were prepared by mixing ligand L with stoichiometric amounts of the hydrated nitrates in THF under ambient conditions. A sequence of precipitation, double re-crystallisation in adequate anhydrous solvents resulted in the isolation of deep red and microcrystalline complexes. The IR spectra of the complexes display a CN stretching band at approximately 1539 cm^{-1} (1545 cm^{-1} for Er), similar to the free-ligand value, indicating little perturbation of the electronic environment of the terpyridine fragment after complexation to the lanthanide salts. The spectra are dominated by strong nitrate vibrations, in particular N–O stretches at 1479–1471 cm^{-1} and 1295–1289 cm^{-1}. Their splitting amounts to 180–190 cm^{-1}, as expected for bidentate coordination mode.[25] A typical example is given in Figure 2.

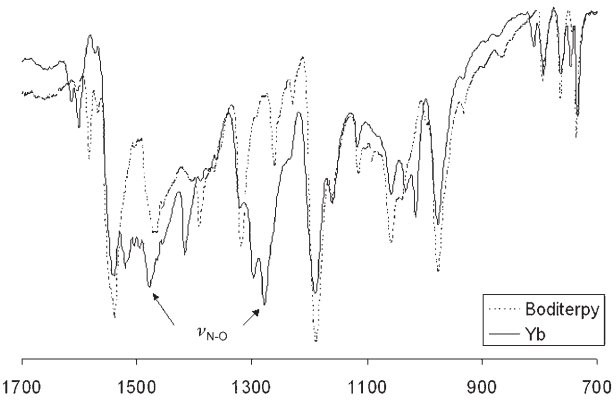

Figure 2. FT-IR spectra of the free ligand and its Yb complex.

Solution study: Electrospray mass spectrometry (ES-MS) provided an insight into the formulation of the complexes in solution. In all cases a molecular peak corresponding to the loss of one nitrate ion (monocation) and a peak due to the loss of a second nitrate ion (dication) were observed. The isotopic distributions of the peaks corresponding to the parent ions unambiguously confirm the monometallic nature of the complexes (Figure 3).

Further information of the solution structure of the complexes was obtained by ^{1}H NMR spectroscopy. Spectra were recorded in various deuterated solvents. In CD_3OD or $CDCl_3$ or mixtures of both, the spectra displayed features typical of a partial decomplexation of the ligands, with

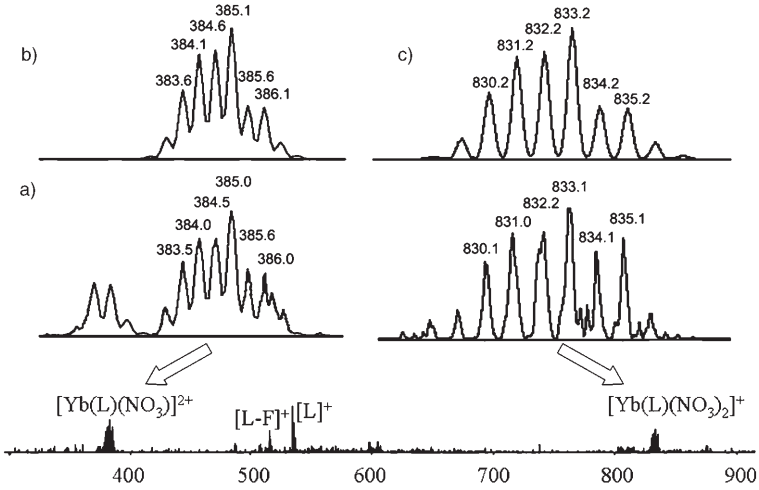

Figure 3. ES-MS spectrum in positive mode at a concentration of *ca* 10^{-5} M in CH_2Cl_2/THF: a) complete spectrum with expansions of the peaks at 385.0 corresponding to the $[Yb(L)(NO_3)]^{2+}$ dication and at 833.1 corresponding to the $[Yb(L)(NO_3)_2]^+$ monocation. b) Computer simulation of the 385.0 peak. c) Computer simulation of the 833.1 peak using the Bruker Daltonics simulate isotopic pattern software.

broadened peaks. In $CDCl_3$, the spectra of the diamagnetic lanthanum complex, displayed two sets of signals arising from the free (14%) and complexed ligand. All signals, including those of the free ligand, are broad, pointing to the presence of a kinetic equilibrium between the species. Only in the case of the weakly polar non-coordinating solvent CD_2Cl_2 was it possible to observe the spectra of the pure complexes. For the La case, the peaks originating from the proton atoms of the boron core are almost unperturbed in their chemical shifts, while important shifts are observed in the aromatic region, principally as a result of the *trans–cis* isomerisation of the pyridine rings.[26] As previously observed upon coordination of Zn^{II},[27] the signals of the lateral pyridine rings are all shifted downfield, while the singlet corresponding to the protons of the central ring is shifted 0.24 ppm upfield when coordinated to La^{III}, due concomitantly to the electron-withdrawing effect of the lanthanum coordination and to the removal of the nitrogen lone pairs of the lateral pyridine rings. As a result of the paramagnetic contribution of the Yb, Nd and Er cations,[28] the ^{1}H NMR spectra of these complexes are considerably broadened and sprayed over few tens of ppm. However, for Ln = Yb, the spectrum, which extends from −5 to +71 ppm, is nicely resolved in CD_2Cl_2 (Figure 4). Interestingly, although the proton signals of the boron-containing moieties are shifted upfield, the hyperfine coupling constants can still be observed. Similarly, some residual hyperfine coupling can be observed for signals at $\delta = 9.30$ (doublet) and 15.26 ppm (broad triplet). On the basis of this spectrum, one can assume that the structure observed in the solid state is maintained in solution with an averaged overall C_{2v} symmetry.

Crystal structure of $[Yb(L)(NO_3)_3]$: Suitable crystals for X-ray investigation were obtained for $[Yb(L)(NO_3)_3]$ by slow diffusion of hexane into a mixture of dichloromethane and diethylether. The nine-coordinate Yb^{III} ion lies in the plane

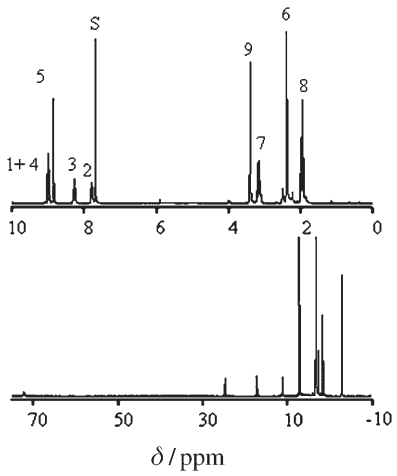

Figure 4. ^{1}H NMR spectra of the free ligand L ($\approx 5\times10^{-3}$ M in $CDCl_3$, top) and of the Yb complex ($\approx 5\times10^{-3}$ M in CD_2Cl_2, bottom). For labelling of the ligand peaks see diagram of ligand. S accounts for $CDCl_3$.

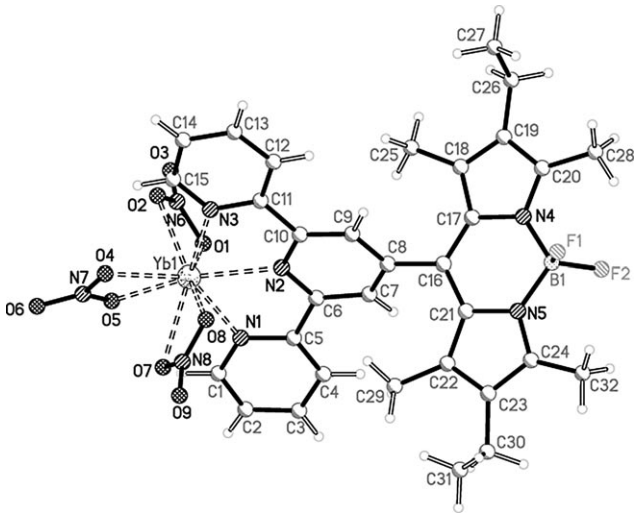

Figure 5. Molecular structure and atom-numbering scheme for [Yb(L)-$(NO_3)_3$].

defined by the nitrogen atoms of the tridentate coordinating unit and its coordination sphere is completed by three bidentate nitrates, leading to a distorted tri-capped antiprism geometry. The nitrates are in pseudo C_{2v} symmetry. Selected bond lengths and angles are given in Table 2, while Figure 5 shows the atom-numbering scheme. As expected, the terpyridine moiety displays an almost planar arrangement, the interplanar angles between the central and the two terminal pyridines being 7.4(2) and 9.8(2)°, respectively. The Yb–N (2.414(4)–2.434(4) Å; average 2.423(11) Å) and Yb–O (2.351(4)–2.511(4) Å; average 2.390(62) Å) distances are standard, as are the N-Yb-N and O-Yb-O bite angles, leading to a calculated ionic radius of the Yb^{III} ion of 1.04(7) Å perfectly in line with the published value for a nine-coordinate complex (1.042 Å).[29]

The terpyridine binding unit is connected to the difluoroboron dipyrromethene moiety by a carbon–carbon bridge (C8–C16) and the interplanar angle between these two parts of the molecule is nearly 60°. The average distances for the boron coordinating site are 1.54(2) and 1.40(11) Å for B–N and B–F, respectively. Weak intra- and intermolecular interactions are observed in the crystal (Figure S2, Supporting Information): 1) intramolecular hydrogen bonds between methyl C28 and fluorine F2 (C···F = 3.033(6) Å; C–H···F = 128°), 2) intermolecular π–π interactions between the terminal pyridines of two adjacent molecules (interplanar distance: 3.62 Å) and 3) intermolecular hydrogen bonding between the aromatic CH bonds and the fluorine atoms or the oxygen atoms of the nitrates (H···X bond; X = O, F; min = 2.36 Å, max = 2.59 Å).

Ligand-centred luminescence: The emission spectra of the ligand and its complexes with nonluminescent lanthanide ions (Ln = La, Gd) in dichloromethane at room temperature are presented in Figure 6. At 295 K, UV excitation in the π→π* and n→π* absorption bands of the ligand (Figure S3 in the Supporting Information) results in a ligand-centred emission displaying one broad band assigned to the $^1\pi\pi^*$ state with maxima at 18180, 18160 and 17986 cm^{-1} for L (Figure S4 in the Supporting Information), $[La(L)(NO_3)_3]$ and $[Gd(L)(NO_3)_3]$, respectively. At 77 K, the singlet-state emission disappears upon enforcement of a time delay (0.1 ms) with concomitant appearance of a broad and weak band arising from the $^3\pi\pi^*$ state emission with maxima between 17450 and 17100 cm^{-1}. The corresponding luminescence decay is a single exponential function of the time corresponding to a $^3\pi\pi^*$-state lifetime of 37 ms for the free ligand, which is lengthened to 41 (Gd) and 52 ms (La) in the complexes (Table 3). The triplet state emission can only be observed in time-resolved mode, because of the large overlap between the fluorescence and

Table 2. Selected bond lengths [Å] and angles [°] in $[Yb(L)(NO_3)_3]$ (standard deviations indicated in parentheses).

bond lengths					
Yb1–O1	2.363(4)	Yb1–O4	2.351(4)	Yb1–O7	2.511(4)
Yb1–O2	2.402(4)	Yb1–O5	2.361(4)	Yb1–O8	2.354(4)
Yb1–N1	2.414(4)	Yb1–N2	2.423(4)	Yb1–N3	2.434(4)
bite angles					
N1-Yb1-N2	66.81(14)	N2-Yb1-N3	66.68(13)	N1-Yb1-N3	133.48(14)
N-Yb-O angles					
O1-Yb1-N1	70.67(14)	O4-Yb1-N1	137.45(13)	N1-Yb1-O7	71.59(14)
O2-Yb1-N1	124.26(15)	O5-Yb1-N1	92.66(13)	O8-Yb1-N1	92.90(15)
O1-Yb1-N2	87.55(13)	O4-Yb1-N2	146.55(14)	N2-Yb1-O7	108.08(12)
O2-Yb1-N2	107.59(13)	O5-Yb1-N2	158.08(14)	O8-Yb1-N2	74.18(13)
O1-Yb1-N3	108.43(14)	O4-Yb1-N3	85.18(13)	N3-Yb1-O7	122.93(13)
O2-Yb1-N3	72.12(14)	O5-Yb1-N3	133.51(13)	O8-Yb1-N3	73.44(13)

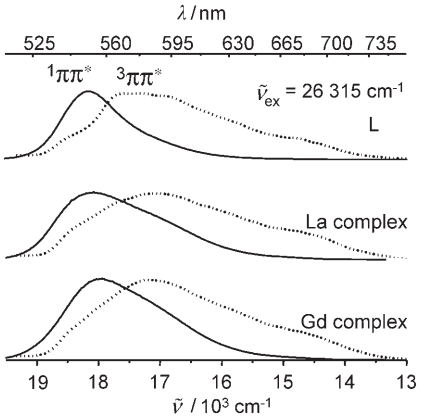

Figure 6. Continuous lines: fluorescence spectra at 295 K of solutions of the ligand and the La^{III} and Gd^{III} complexes in dichloromethane. Dotted lines: phosphorescence spectra at 77 K, delay = 0.1 ms. Spectra are normalised and not drawn on the same vertical scale.

Table 3. Absolute quantum yields [%] of the ligand-centred fluorescence at 298 K in dichloromethane (ν_{ex} = 20491 cm^{-1}) and lifetimes of the ligand $^3\pi\pi^*$ state (the analysing wavelength was set on the maximum of the ligand $^3\pi\pi^*$ emission).

Compound	τ [ms]	$Q^{1\pi\pi^*}$ [%]
L	37 ± 2	79 ± 8
[La(L)(NO$_3$)$_3$]	52 ± 3	54 ± 5
[Nd(L)(NO$_3$)$_3$]		15 ± 2
[Gd(L)(NO$_3$)$_3$]	41 ± 3	21 ± 3
[Er(L)(NO$_3$)$_3$]		20 ± 2
[Yb(L)(NO$_3$)$_3$]		19 ± 2

phosphorescence bands. Therefore, it is difficult to estimate the efficiency of the intersystem crossing; we note, however, that the energy gap between the 0-phonon transitions of the two states is quite small, $\Delta E(^1\pi\pi^* - ^3\pi\pi^*) = 660$ cm^{-1}, while a value of 5000 cm^{-1} is usually considered as being optimum.

The strong emission from the ligand $^1\pi\pi^*$ state, centred about 18000 cm^{-1}, is independent of the excitation energy and observed for all the complexes in dichloromethane solution (Ln = Nd, Er, Yb, Figure S5 in the Supporting Information). The fluorescence quantum yields have been determined with respect to the Rhodamine 6G standard under excitation at 488 nm and are listed in Table 3.

Sensitisation of lanthanide-centred NIR emission: The [Ln(L)(NO$_3$)$_3$] complexes with Ln = Nd, Er, and Yb display metal-centred luminescence. In a first step, we analysed the transition of solid-state samples both at room temperature, and 10 K in order to gain information on the photophysics of these compounds. At the latter temperature, the luminescence spectrum of the [Nd(L)(NO$_3$)$_3$] complex, under excitation at 19455 cm^{-1} by the Ar-laser line, displays three NIR bands in the spectral ranges 11800–10600, 9700–9200 (main component) and 7700–7000 cm^{-1} (Figure 7 and Figures S6, S7, in the Supporting Information). They are composed of 4, 5 and 7 main components, respectively, and are assigned to

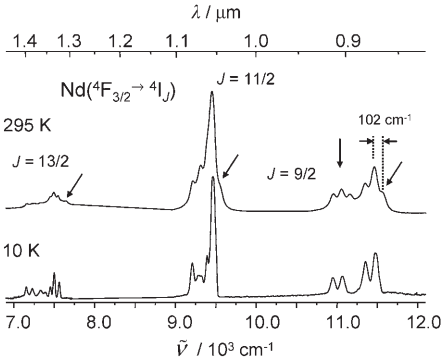

Figure 7. Emission spectra of the [Nd(L)(NO$_3$)$_3$] complex ($^4F_{3/2} \rightarrow {}^4I_{9/2}$, $^4I_{11/2}$ and $^4I_{13/2}$ transitions) in the solid state at 10 and 295 K; arrows denote "hot" bands (see text).

transitions from the $^4F_{3/2}$ level to the $^4I_{9/2}$, $^4I_{11/2}$ and $^4I_{13/2}$ sublevels, respectively, and the number of main crystal-field components (4, 5 and 7, respectively) points to a low site symmetry for the metal ion, the maximum degeneracy being 5, 6 and 7, respectively. The relative corrected and integrated intensities of the Nd($^4F_{3/2} \rightarrow {}^4I_{j/2}$) transitions are reported in Table S1 (in the Supporting Information). Upon increasing the temperature from 10 to 295 K, the emission spectra become broader, but the energy difference between the components of the transitions is not affected. However, the spectra display additional bands on the high energy side of the components observed at low temperature. At room temperature, the three NIR bands are still visible and display 6, 5 and 8 components, respectively. We interpret these additional emission bands as being "hot" bands arising from a crystal-field sublevel of $^4F_{3/2}$ with higher energy (+102 cm^{-1}, see Figure 7 and Figure S5 in the Supporting Information).

At 10 K, the luminescence of the [Yb(L)(NO$_3$)$_3$] complex is characterised by several peaks in the range 10600–9300 cm^{-1} (Figure 8), which are assigned to the $^2F_{5/2} \rightarrow {}^2F_{7/2}$ transition and arise from the M_J splitting of the ground and/or emitting states, since six transitions are observed while the degeneracy of the $^2F_{7/2}$ level is four (Kramer's doublets).

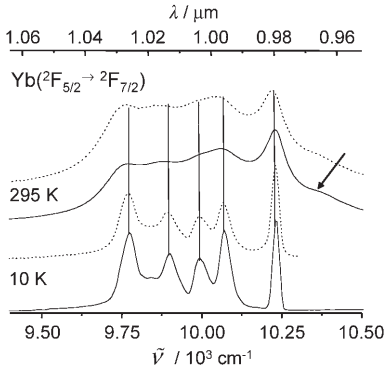

Figure 8. Emission spectra of the [Yb(L)(NO$_3$)$_3$] complex at 10 and 295 K (ν_{ex} = 19 455 cm^{-1}); solid line: powdered sample, dotted line: single crystals used for the X-ray study; the arrow points to a "hot" band.

At 295 K, the overall shape of the spectrum and the crystal-field splitting remain the same, but for the expected broadening and for the appearance of an additional component at higher energy, again due to emission from a thermally populated higher crystal-field sublevel of $^2F_{5/2}$ ($+138\ cm^{-1}$). We have also checked that the sample preparation does not influence the emission properties in recording the luminescence spectra of the single crystals used for X-ray structural study (Figure 8). From the various crystal-field sublevels identified (Table S2, Supporting Information), one sees that the total splitting is of $455\ cm^{-1}$. As a comparison, for a Yb complex in a low symmetry a value of $528\ cm^{-1}$ has been found and a smaller total splitting of $372\ cm^{-1}$ has been reported for a D_3-symmetrical bimetallic helicate[30] (in line with the higher symmetry of the metal ion site). Here, the value is consistent with a low-symmetry environment around the metal ion.

The luminescence decays of the Nd($^4F_{3/2}$) and Yb($^2F_{5/2}$) states, measured on solid-state samples at 10 K and upon excitation through the ligand $^1\pi\pi^*$ level, are single exponential functions, indicating a fast energy transfer from the ligand to the metal ion[8] and also the presence of efficient nonradiative deactivation processes, since they are much shorter than the radiative lifetimes (Table 4).

Table 4. Lifetimes of the Nd($^4F_{3/2}$) and Yb($^2F_{5/2}$) excited levels in the [Ln(L)$(NO_3)_3$] complexes under various excitation conditions (solid state), absolute quantum yields of solutions 10^{-4}–10^{-7} M in dichloromethane, and estimated sensitisation efficiency (see text).

T [K]	Complex	ν_{an} [cm^{-1}]	τ [μs]	Q^L_{Ln} [%]	$Q^{Ln}_{Ln}(\frac{\tau_{obs}}{\tau_{rad}})$ [%]	η_{sens}
10	[Nd(L)$(NO_3)_3$]	11481	0.20(2)			
	[Yb(L)$(NO_3)_3$]	10225	11.1(2)			
295	[Nd(L)$(NO_3)_3$]	11560	0.27(2)	$1.6(2)\times10^{-2}$	3.38×10^{-2}	0.47
	[Yb(L)$(NO_3)_3$]	10225	9.7(1)	0.31(3)	0.49	0.63

Finally, the [Er(L)$(NO_3)_3$] complex proved to be very weakly luminescent, although its characteristic band at $6550\ cm^{-1}$ could be observed, but its decay time could not be measured. (Figures S6 and S8, in the Supporting Information).

In a second step, we investigated solutions of the complexes in dichloromethane (10^{-4} M), both from structural and quantitative viewpoints. The corresponding emission spectra are very similar, at least with respect to crystal-field splitting, to those observed in the solid state, except for the expected broadening (Figures S9 and S10, in the Supporting Information). Therefore, the chemical environment of the metal ions must be very similar in both media, which also translates into similar lifetimes for solutions, within experimental errors, relative to solid-state samples.

The absolute quantum yields of the luminescence of the Nd($^4F_{3/2}$) and Yb($^2F_{5/2}$) levels in the [Ln(L)$(NO_3)_3$] complexes have been measured upon ligand excitation (18657–18727 cm^{-1}) by using [Yb(tta)$_3$(H_2O)$_2$] as reference.[24] A value of 0.31 ± 0.03% has been obtained for the [Yb(L)-$(NO_3)_3$] complex, which is reasonably large with respect to other published data, for instance 1.8% for a bimetallic helicate in D_2O,[30] 0.45% for the complex with fluorexon in D_2O,[31] 0.5% for a terphenyl-based complex in DMSO,[32] or 0.23, 0.14 and 0.17% for complexes with fluorescein, eosin and erythrosin, respectively, in deuterated methanol.[33] Although small, the quantum yield of the [Nd(L)$(NO_3)_3$] complex, $(1.6\pm0.2)\times10^{-2}$%, can also be considered as being interesting if compared with 3.8×10^{-2}% for the Nd–fluorexon complex in D_2O[31] and with $3.0\cdot10^{-2}$, $1.4\cdot10^{-2}$ and $1.2\cdot10^{-2}$% for Nd^{III} complexes with fluorescein, eosin and erythrosin, respectively, in deuterated methanol.[33]

The overall quantum yield Q^L_{Ln} of a luminescent Ln^{III} chelate, upon ligand excitation, is given by Equation (2) in which η_{sens} is the efficiency of the overall ligand-to-metal energy transfer, η_{isc} the efficiency of the intersystem crossing, η_{et} the efficacy of the $^3\pi\pi^*$–Ln energy transfer, and Q^{Ln}_{Ln} the intrinsic quantum yield, that is, the quantum yield obtained upon direct Ln^{III} excitation.

$$Q^L_{Ln} = \eta_{sens}\, Q^{Ln}_{Ln} = \eta_{isc}\, \eta_{et}\, Q^{Ln}_{Ln} = \eta_{isc}\, \eta_{et}\, \frac{\tau_{obs}}{\tau_{rad}} \qquad (2)$$

The Q^{Ln}_{Ln} parameter is much influenced by the presence of high-energy vibrations in the inner coordination sphere (and also in the neighbourhood of the ion). Estimates of τ_{rad} in organic systems have been published to be 0.8 and 2 ms, for Nd^{III} and Yb^{III}, respectively[34] and taking these figures into account, we can estimate $\eta_{sens}=0.48$ and 0.63 for the Nd^{III} and Yb^{III} complexes, respectively.

Conclusion

To summarise, new lanthanide complexes bearing a terpyridine ligand, with a strong absorbing unit attached, and three coordinated nitrate anions have been prepared and fully characterised, including a X-ray crystal structure in the case of Yb^{III}. The investigated complexes, particularly [Nd(L)-$(NO_3)_3$] and [Yb(L)$(NO_3)_3$], display a sizeable NIR luminescence both in solid state and in solution, probably occurring by energy transfer from the appended boron fragment. Whereas the designed ligand can be considered as being an interesting sensitiser of Nd^{III} and Yb^{III} luminescence, the Er^{III} complex has proved to be only very weakly luminescent, either because of efficient nonradiative deactivation processes or because of inefficient energy transfer from boditerpy ligand. Indeed the energy difference between the ligand triplet state and the excited-state levels of Er^{III} is less favourable to an efficient energy transfer than in the case of the two other ions. However, in absence of quantitative data due to the faint emission of the Er^{III} complex, the exact reason for this poor sensitisation could not be determined.

The next step in this research program will be to increase the stability of the resulting complexes by adding negatively charged fragments on the chelating core. Also under active investigation is the engineering of boron fragments absorb-

ing and emitting more intensely at longer wavelength in order to benefit from a more efficient antenna effect and to favour energy transfer from the organic core to the emissive states of the lanthanide ions. This could for instance involve a positioning of the indacene unit closer to the acceptor metal ion, and in a more favourable orientation for energy transfer, for instance by designing three-dimensional coordination polymers containing these building blocks.

Acknowledgements

This research is supported through grants from the Swiss National Science Foundation and by the French Centre National de la Recherche Scientifique. We thank Mr. Frédéric Gumy for his help in luminescence measurements.

[1] R. Weissleder, V. Ntziachristos, *Nat. Med.* **2003**, *9*, 123–128.
[2] S. Faulkner, S. J. A. Pope, B. P. Burton-Pye, *Appl. Spectrosc. Rev.* **2005**, *40*, 1–31.
[3] G. A. Hebbink, J. W. Stouwdam, D. N. Reinhoudt, F. C. J. M. Van Veggel, *Adv. Mater.* **2002**, *14*, 1147–1150.
[4] T. S. Kang, B. S. Harrison, M. Bouguettaya, T. J. Foley, J. M. Boncella, K. S. Schanze, J. R. Reynolds, *Adv. Funct. Mater.* **2003**, *13*, 205–210.
[5] J.-C. G. Bünzli, C. Piguet, *Chem. Soc. Rev.* **2005**, *34*, 1048–1077.
[6] a) M. Latva, H. Takalo, V.-M. Mukkala, C. Matachescu, J. C. Rodriguez-Ubis, J. Kankare, *J. Lumin.* **1997**, *75*, 149–169; b) F. J. Steemers, W. Verboom, D. N. Reinhoudt, E. B. van der Tol, J. W. Verhoeven, *J. Am. Chem. Soc.* **1995**, *117*, 9408–9414.
[7] a) G. A. Hebbink, S. I. Klink, L. Grave, P. G. B. Oude Alink, F. C. J. M. van Veggel, *ChemPhysChem* **2002**, *3*, 1014–1018; b) V. Vicinelli, P. Ceroni, M. Maestri, V. Balzani, M. Gorka, F. Vögtle, *J. Am. Chem. Soc.* **2002**, *124*, 6461–6468; c) C. Yang, L.-M. Fu, Y. Wang, J.-P. Zhang, W.-T. Wong, X.-C. Ai, Y.-F. Qiao, B.-S. Zou, L.-L. Gui, *Angew. Chem.* **2004**, *116*, 5120–5123; *Angew. Chem. Int. Ed.* **2004**, *43*, 5010–5013.
[8] S. Torelli, D. Imbert, M. Cantuel, G. Bernardinelli, S. Delahaye, A. Hauser, J.-C. G. Bünzli, C. Piguet, *Chem. Eur. J.* **2005**, *11*, 3228–3242.
[9] D. Imbert, M. Cantuel, J.-C. G. Bünzli, G. Bernardinelli, C. Piguet, *J. Am. Chem. Soc.* **2003**, *125*, 15698–15699.
[10] a) S. J. A. Pope, B. J. Coe, S. Faulkner, E. V. Bichenkova, X. Yu, K. T. Dougla, *J. Am. Chem. Soc.* **2004**, *126*, 9490–9491; b) S. I. Klink, H. Keizer, F. C. J. M. van Veggel, *Angew. Chem.* **2000**, *112*, 4489–4491; *Angew. Chem. Int. Ed.* **2000**, *39*, 4319–4321.
[11] a) D. Imbert, S. Comby, A.-S. Chauvin, J.-C. G. Bünzli, *Chem. Commun.* **2005**, 1432–1434; b) S. Comby, D. Imbert, A.-S. Chauvin, J.-C. G. Bünzli, *Inorg. Chem.* **2006**, *45*, 732–743.
[12] a) B. S. Harrison, T. J. Foley, A. F. Knefely, J. K. Mwaura, G. B. Cunningham, T.-S. Kang, M. Bouguettaya, J. M. Boncella, J. R. Reynolds, K. Schanze, *Chem. Mater.* **2004**, *16*, 2938–2947; b) T. J. Foley, B. S. Harrison, A. S. Knefely, K. A. Abboud, J. R. Reynolds, K. S. Schanze, J. M. Boncella, *Inorg. Chem.* **2003**, *42*, 5023–5032.
[13] G. A. Hebbink, D. N. Reinhoudt, F. C. J. M. van Veggel, *Eur. J. Org. Chem.* **2001**, 4101–4106.
[14] S. Faulkner, M.-C. Carrié, S. J. A. Pope, J. Squire, A. Beeby, P. G. Sammes, *Dalton Trans.* **2004**, 1405–1409.
[15] B. P. Burton-Pye, S. L. Heath, S. Faulkner, *Dalton Trans.* **2005**, 146–149.
[16] a) M. H. V. Werts, J. W. Hofstraat, F. A. J. Geurts, J. W. Verhoeven, *Chem. Phys. Lett.* **1997**, *276*, 196–201; b) M. H. V. Werts, R. H. Woudenberg, P. G. Emmerink, R. van Gassel, J. W. Hofstraat, J. W. Verhoeven, *Angew. Chem.* **2000**, *112*, 4716–4718; *Angew. Chem. Int. Ed.* **2000**, *39*, 4542–4544.
[17] C. Goze, G. Ulrich, L. Charbonnière, R. Ziessel, *Chem. Eur. J.* **2003**, *9*, 3748–3755.
[18] M. Galletta, S. Campagna, M. Quesada, G. Ulrich, R. Ziessel, *Chem. Commun.* **2005**, 4222–4224.
[19] Oxford Diffraction, Abingdon, Oxfordshire, OX14 1RL (UK), **2003**.
[20] N. Walker, D. Stuart, *Acta Crystallogr. Sect. A* **1983**, *A39*, 158–166.
[21] a) G. M. Sheldrick, *Acta Crystallogr. Sect. A* **1990**, *46*, 467–473; b) SHELXTL Release 5.1, Bruker AXS Inc., Madison, Wisconsin, 53719 (USA), **1997**.
[22] R. Rodriguez-Cortinas, F. Avecilla, C. Platas-Iglesias, D. Imbert, J.-C. G. Bünzli, A. de Blas, T. Rodriguez-Blas, *Inorg. Chem.* **2002**, *41*, 5336–5349.
[23] J. Olmsted III, *J. Phys. Chem.* **1979**, *83*, 2581–2594.
[24] S. B. Meshkova, Z. M. Topilova, D. V. Bolshoy, S. V. Beltyukova, M. P. Tsvirko, V. Y. Venchikov, V. Ya, *Acta Phys. Pol. A* **1999**, *95*, 983–990.
[25] a) N. F. Curtis, Y. M. Curtis, *Inorg. Chem.* **1965**, *4*, 804–809; b) J. Fawcett, A. W. G. Platt, S. Vickers, M. D. Ward, *Polyhedron* **2004**, *23*, 2561–2567.
[26] S. Comby, D. Imbert, A.-S. Chauvin, J.-C. G. Bünzli, L. J. Charbonnière, R. F. Ziessel, *Inorg. Chem.* **2004**, *43*, 7369–7379.
[27] A. Harriman, J. P. Rostron, M. Cesario, G. Ulrich, R. Ziessel, unpublished results.
[28] a) I. Bertini, P. Turano, A. J. Vila, *Chem. Rev.* **1993**, *93*, 2833–2932; b) J. Lisowski, J. L. Sessler, V. Lynch, T. D. Mody, *J. Am. Chem. Soc.* **1995**, *117*, 2273–2285; c) M. Elhabiri, R. Scopelliti, J.-C. G. Bünzli, C. Piguet, *J. Am. Chem. Soc.* **1999**, *121*, 10747–10762.
[29] G. R. Choppin in *Lanthanide Probes in Life, Chemical and Earth Sciences*, (Eds.: J.-C. G. Bünzli, G. R. Choppin), Elsevier, Amsterdam **1989**, Chapter 1.
[30] F. R. Gonçalves Silva, O. L. Malta, C. Reinhard, H. U. Güdel, C. Piguet, J. E. Moser, J.-C. Bünzli, *J. Phys. Chem. A* **2002**, *106*, 1670–1677.
[31] M. H. V. Werts, J. W. Verhoeven, J. W. Hofstraat, *J. Chem. Soc. Perkin Trans. 2* **2000**, 433–439.
[32] S. I. Klink, G. A. Hebbink, L. Grave, F. C. J. M. Van Veggel, D. N. Reinhoudt, L. H. Sloof, A. Polman, J. W. Hofstraat, *J. Appl. Phys.* **1999**, *86*, 1181–1185.
[33] G. A. Hebbink, L. Grave, L. A. Woldering, D. N. Reinhoudt, F. C. J. M. van Veggel, *J. Phys. Chem. A* **2003**, *107*, 2483–2491.
[34] J. W. Hofstraat, M. P. Oude Wolbers, F. C. J. M. van Veggel, D. N. Reinhoudt, M. H. V. Werts, J. W. Verhoeven, *J. Fluoresc.* **1998**, *8*, 301–308.

Received: January 27, 2006
Published online: April 25, 2006

